Schizophrenia Research 248 (2022) 107–113

Contents lists available at ScienceDirect

Schizophrenia Research

journal homepage: www.elsevier.com/locate/schres

Neuroanatomical subtypes of schizophrenia and relationship with illness duration and deficit status

Qian Hui Chew [a,1], K.N. Bhanu Prakash [b,d,1], Li Yang Koh [b], Geetha Chilla [b,d], Ling Yun Yeow [b,d], Kang Sim [c,*]

[a] Research Division, Institute of Mental Health, Singapore
[b] Biophotonics & Bioimaging, Institute of Bioengineering and Bioimaging, Agency for Science, Technology and Research, Singapore
[c] West Region, Institute of Mental Health, Singapore
[d] Clinical Data Analytics & Radiomics, Bioinformatics Institute, Agency for Science, Technology and Research, Singapore

ARTICLE INFO

Keywords:
Neuroimaging
Schizophrenia
Subtypes

ABSTRACT

Background: The heterogeneity of schizophrenia (SCZ) regarding psychopathology, illness trajectory and their inter-relationships with underlying neural substrates remain incompletely understood. In a bid to reduce illness heterogeneity using neural substrates, our study aimed to replicate the findings of an earlier study by Chand et al. (2020). We employed brain structural measures for subtyping SCZ patients, and evaluate each subtype's relationship with clinical features such as illness duration, psychotic psychopathology, and additionally deficit status.

Methods: Overall, 240 subjects (160 SCZ patients, 80 healthy controls) were recruited for this study. The participants underwent brain structural magnetic resonance imaging scans and clinical rating using the Positive and Negative Syndrome Scale. Neuroanatomical subtypes of SCZ were identified using "Heterogeneity through discriminative analysis" (HYDRA), a clustering technique which accounted for relevant covariates and the inter-group normalized percentage changes in brain volume were also calculated.

Results: As replicated, two neuroanatomical subtypes (SG-1 and SG-2) were found amongst our patients with SCZ. The subtype SG-1 was associated with enlargements in the third and lateral ventricles, volume increase in the basal ganglia (putamen, caudate, pallidum), longer illness duration, and deficit status. The subtype SG-2 was associated with reductions of cortical and subcortical structures (hippocampus, thalamus, basal ganglia).

Conclusions: These replicated findings have clinical implications in the early intervention, response monitoring, and prognostication of SCZ. Future studies may adopt a multi-modal neuroimaging approach to enhance insights into the neurobiological composition of relevant subtypes.

1. Introduction

Schizophrenia (SCZ) is a chronic and serious mental illness affecting >27 million worldwide (GBD 2017 Disease and Injury Incidence and Prevalence Collaborators, 2018). Heterogeneity in neurobiology (Voineskos et al., 2020), polygenic scores (Alnæs et al., 2019), symptom presentations (Van Rheenen et al., 2017), treatment responses (Malhotra, 2015), and outcomes (Huber, 1997) and their inter-relationships remain incompletely understood and can potentially confound evaluation and affect management of the condition (Lakhan and Vieira, 2009). Grouping patients by clinical subtypes allows for a deeper examination of homogenous groups, and this is often done using measures which assess symptomatology (e.g positive/negative symptom domains), cognitive status or illness course (e.g remission status) (Tan et al., 2020; Weinberg et al., 2016; Wong et al., 2020). Previous studies have attempted to link these clinical subtypes in SCZ based on deficit syndrome (Tan et al., 2020), cognitive functioning (Ho et al., 2020; Seaton et al., 2001; Weinberg et al., 2016) and remission status (Wong

Abbreviations: ARI, Adjusted rand index; DS, Deficit syndrome; GAF, Global Assessment of Functioning; HC, Healthy controls; HYDRA, Heterogeneity through discriminative analysis; PANSS, Positive and Negative Syndrome Scale; SCZ, Schizophrenia.

* Corresponding author at: Institute of Mental Health, 10, Buangkok View, Singapore 539747, Singapore.
E-mail address: kang_sim@imh.com.sg (K. Sim).

[1] Joint first authors.

https://doi.org/10.1016/j.schres.2022.08.004
Received 3 February 2022; Received in revised form 21 July 2022; Accepted 15 August 2022
Available online 25 August 2022

et al., 2020) with underlying neural substrates.

Recent advances in the field of machine learning have facilitated the application of neuroimaging-based measures for the classification of patients with SCZ and healthy controls (HCs) (Chand et al., 2020; Chin et al., 2018; Hu et al., 2021; Oh et al., 2019) and the evaluation of underlying brain changes in SCZ (Ivleva et al., 2012; Killgore et al., 2009; Pina-Camacho et al., 2016; Womer et al., 2014). Using neuroanatomical substrates to group SCZ could potentially highlight biological subtypes which can be correlated with clinical features. Evaluation of these neural subtypes could allow for monitoring of biological changes and responses to treatment and can help in management and prognostication of patients (Dwyer et al., 2018; Voineskos et al., 2020). Thus far, compared with clinical subtyping, there are fewer studies which have explored neuroanatomical subtyping and its relationship with other relevant clinical features (Chand et al., 2020; Dwyer et al., 2018). Additionally, amongst these studies, the process of subtyping was carried out only using neuroanatomical features within the patient group without the inclusion of other confounding variables such as age and gender which can influence subtyping results (Arnedo et al., 2015; Clementz et al., 2016; Du et al., 2015). In this regard, a novel method known as HYDRA (heterogeneity through discriminative analysis) (Varol et al., 2017) can be used as it models differences between patient subtypes as well as HCs based on neuroanatomical features and relevant covariates.

In a bid to reduce illness heterogeneity using neural substrates, we aimed to replicate the earlier findings by Chand et al. (2020). We carried out clustering of HCs and SCZ subtypes simultaneously using HYDRA and evaluated the relationship between SCZ subtypes with clinical features such as illness duration, psychotic psychopathology and additionally deficit status.

2. Materials and methods

2.1. Study sample

We recruited patients with SCZ and HCs from the Institute of Mental Health, Singapore, and the community respectively. Patients with SCZ were diagnosed using structured clinical interviews of the Diagnostic and Statistical Manual of Mental Disorders, Fourth Edition diagnostic criteria (DSM-IV)-Patient Version (First et al., 1994a, 1994b), with information from the comprehensive clinical history, mental state examination, and existing medical records. All patients had no history of any significant neurological illness such as seizures, cerebrovascular accidents, or head injury. The HCs had no history of psychiatric or neurological disorders (based on the Structured Clinical Interview for Diagnosis, nonpatient version) (First et al., 1994b) and were not receiving any psychotropic medications. Written, informed consent was obtained from all the participants after a detailed explanation of the study procedures. The study protocol was approved by the Institutional Review Boards of both the Institute of Mental Health and the National Healthcare Group, Singapore (NHG DSRB Ref: 05/00186, 07/00102).

2.2. Clinical evaluations

The Positive and Negative Syndrome Scale (PANSS) (Kay et al., 1987) was administered to assess the severity of psychopathology and the Global Assessment of Functioning (GAF; APA, 1994) was used to measure the level of psychosocial functioning. For the deficit status, we used the Proxy for the Deficit Syndrome (PDS) criteria (Kirkpatrick et al., 1993) to identify patients with Deficit Syndrome (DS). The PDS is a valid tool for the categorization of deficit and non-deficit SCZ (Goetz et al., 2007). The PDS is defined as the sum of the PANSS items for anxiety, guilt, depressive mood, and hostility subtracted from the blunted affect item score i.e. PDS index score $=\sum$Blunted affect(N1) – [Anxiety(G2) + Guilt feelings(G3) + Depression(G6) + Hostility(P7)]. As with previous studies (Sum et al., 2018; Voineskos et al., 2013), an index cut-off point of −2 was used to classify deficit versus non-deficit patients. To ensure the stability of the diagnosis, the negative symptoms had to be present for at least a year (Fenton and McGlashan, 1994) as determined by the clinician investigator when assessing the presence and severity of negative symptoms.

2.3. Neuroimaging using MRI and image processing

All images were acquired on a 3-Tesla MR system (Achieva 3 T, Philips Medical Systems, Eindhoven, Netherlands) with the whole brain, high resolution, 3D MP-RAGE (magnetization-prepared rapid acquisition with a gradient echo) volumetric scans (TR/TE/TI/flip angle 8.4/3.8/3000/8; matrix 256 × 204; FOV 240 mm2) with axial orientation (reformatted to coronal), and covering the whole brain for structural-anatomic detail.

FreeSurfer 6.0.0 was used for neuroimage processing and to extract cortical parcellation parameters from structural MRI data. This was performed by following a 5 step pre-processing protocol (fully described in (Fischl et al., 2004; Fischl et al., 1999)), which were (i) Affine registration with MNI305 space (ii) Volumetric labeling, (iii) B1 bias field correction, and (iv) High dimensional nonlinear volumetric alignment to the MNI305 atlas and (v) Subcortical segmentation/cortical parcellation. After the pre-processing steps, the data are labeled via a final segmentation step that is based on both subject-independent probabilistic atlas and subject-specific measured values. The processing pipeline was conducted via a docker and singularity-based framework of the parallel multi-GPU-based computing environment at the National Supercomputing Center, Singapore.

2.4. Identifying neuroanatomical subtypes using HYDRA

Neuroanatomical subtypes in SCZ were identified using "Heterogeneity through discriminative analysis" (HYDRA) (Varol et al., 2017), a clustering technique with neuroimaging features as input factors and which takes into account relevant covariates such as age, gender, antipsychotic dose. HYDRA is a multivariate simultaneous classification and clustering technique (Varol et al., 2017) which separates HC and SCZ patients by building a convex polytope with maximum margins around the control group samples. Each face of the polytope identifies the subtypes in the patient group. HYDRA is different from other clustering techniques (e.g. k-means, fuzzy c-means, nearest neighbors) as it uses imaging feature differences for subtyping. The associations of SCZ subjects to the facets of the polytope determine their membership to different illness subtypes. The optimal number of subtypes is identified by calculating either the "Rand Index", a measure of similarity between clusters, or by using "Adjusted Rand Index (ARI)", which takes into account the chance of grouping the elements into clusters, correlations between regions and indicates the accuracy of groupings. The subtyping index (k) varied from 2 to 10 and adjusted rand index (ARI) (Varol et al., 2017) was calculated to identify the optimal number of subtypes in our study sample.

2.5. Statistical analysis

R studio version R-4.0.3 (R Core Team, 2020; R Studio Team, 2020) was used to perform comparisons of structural volumes between SCZ, HC and SCZ subtypes. The statistical package JMP12®, a statistical division of SAS (JMP, 1989-2021), was used for all the Generalized Linear Model (GLM) based model analyses in the study. The "Fit model" function, was used to calculate the various GLM fits to specify the distributions and their respective link functions. The inter-group normalized percentage changes in brain volume (SCZ, SCZ subtypes and HC) were calculated using the formula $\%Volume\ change = \frac{(Volume_{HC} - Volume_{SG})}{\frac{(Volume_{HC} + Volume_{SG})}{2}} * 100$.

3. Results

3.1. Overall sample

Overall, 240 subjects (SCZ = 160, HC = 80) participated in this study. Quality check of the subject MRI data revealed imaging artifacts in 2 SCZ and 4 HC subjects which were subsequently excluded from the analysis, thus leaving a final data set of 234 subjects (SCZ = 158, HC = 76). In terms of demographic characteristics of the study cohort, SCZ and HC were comparable in age and gender (Table 1).

3.2. Neuroanatomical subtypes identified using HYDRA

The number of neuroanatomical subtypes (k) in HYDRA (Varol et al., 2017), yielded the highest adjusted rand index (ARI) for k = 2, indicating the optimal number of subtypes which were labeled as subtypes SG-1 and SG-2. Furthermore, the efficacy of HYDRA's clustering was evaluated by changing the order of the variables, and by using a subset of the variables. <1 % of interchange was observed between subtypes implying the robustness of HYDRA-based clustering and classification.

The clinical and demographic characteristics of the subtypes (SG-1 & SG-2) are summarised in Table 2. The 2 subtypes differed in terms of illness duration (SG-1 > SG-2, $p < 0.001$) but were comparable in terms of age, gender, PANSS total, and GAF scores. The distribution of deficit/non deficit status amongst the 2 subtypes was 33.3 %/66.7 % for SG-1, and 16.9 %/83.1 % for SG-2 respectively, and SG-1 was associated with a greater proportion of subjects with deficit status (χ^2 (1158) = 5.49, p = 0.019).

In terms of normalized percentage brain volume differences, compared with HC, subtype SG-1 showed an increase in brain volumes involving lateral ventricles and basal ganglia whilst subtype SG-2 showed a decrease in brain volumes involving cortical and subcortical structures (hippocampus, thalamus, basal ganglia) (Fig. 1). Of note, reduced volumes of corpus callosum (central, mid-anterior and mid-posterior portions) are found in both neuroanatomical subtypes SG-1 and SG-2.

4. Discussion

There were several main findings from our study. First, we replicated the two main neuroanatomical subtypes described in Chand et al. (2020) within our population of patients with SCZ. Second, in this study, the subtype SG-1 was associated with brain volume enlargements in the third and lateral ventricles, basal ganglia (putamen, caudate, pallidum), longer illness duration, and deficit status. The subtype SG-2 was associated with brain volume reductions of cortical and subcortical structures (hippocampus, thalamus, basal ganglia). In addition, volume reductions of corpus callosum were seen in both neuroanatomical subtypes.

SCZ subtype SG-1 was associated with illness chronicity, and deficit status but not SG-2. The biological findings related to the two subtypes extended the clinical two-syndrome concept postulated by Crow (1985) whereby Type II SCZ was characterized by deficit symptoms, poorer response to neuroleptics, and potentially irreversible psychosis and symptoms. Type I SCZ, on the other hand, was characterized by absence of deficit status, better response to neuroleptics, and potentially reversible psychosis and symptoms. Thus, SG-1 subtype in our study corresponded to Crow's Type II SCZ (longer duration of illness, deficit status) and was associated with enlargements of the third and lateral ventricles, as well as the basal ganglia. Ventricular enlargement has been previously suggested to indirectly reflect changes in the temporal lobe over time (Brown et al., 1986) and basal ganglia enlargement is thought to be a response to antipsychotic treatment longitudinally (Borgwardt et al., 2009). Subtype SG-2 in this study corresponded with Crow's Type I SCZ (absence of deficit status), and was associated with specific brain changes, namely, volume reductions of cortical and subcortical structures (hippocampus, thalamus, basal ganglia).

We found that subtype SG-1 was associated with deficit status. This is consistent with earlier literature which found an association between deficit symptoms and enlargements of the third and lateral ventricles as seen in subtype SG-1 (Andreasen et al., 1982; Weinberger et al., 1979). Third ventricular width has been postulated to be related to the mode of onset of SCZ in one study (Sandyk, 1993), as a greater width was associated with an insidious onset and less favourable outcome. Deficit status can be debilitating and are associated with motivational deficits which are related to underlying basal ganglia changes (Goldsmith and Rapaport, 2020). Apart from motor functioning, the basal ganglia is thought to play a role in emotional processing, and has been implicated in affective flattening (Bragulat et al., 2007) and anhedonia (Dunn et al., 2002; Plailly et al., 2006) in clinical populations. Ballmaier and colleagues (2008) found an inverse relationship between volume changes in the anterior pole of the putamen and severity of blunted affect in unmedicated patients with SCZ. Whilst previous studies had reported basal ganglia enlargements with chronicity of illness and treatment (Okada et al., 2016; van Erp et al., 2016), a recent meta-analysis

Table 1
Demographic and clinical characteristics of study cohort.

Features	HC (N = 76)	SCZ (N = 158)	Statistical test
Age, years, mean ± SD	32.82 ± 9.11	33.3 ± 9.0	*t*-stat = −0.39, *df* = 344.88, p = 0.70
Gender, Males, n (%)	47 (61.8 %)	107 (67.7 %)	χ^2 (1, 234) = 0.79, *p* = 0.37
Age at illness onset, years	–	26.16 ± 7.57	–
Illness duration, years	–	6.49 ± 7.36	–
Antipsychotic dose, CPZ eq mg/day	–	206.47 ± 185.26	–
PANSS total score	–	40.4 ± 8.9	–
GAF total score	–	50.9 ± 18.2	–

Abbreviations: CPZ eq = Chlorpromazine equivalents; GAF = Global Assessment of Functioning; HC = Healthy controls;
PANSS = Positive and Negative Syndrome Scale; SCZ = Schizophrenia.

Table 2
Demographic and clinical characteristics of neuroanatomical subtypes SG-1 and SG-2.

Feature	SCZ (N = 158)	SG-1 (N = 87)	SG-2 (N = 71)	SG-1 vs SG-2
Age, years, mean ± SD	33.3 ± 9.0	34.80 ± 8.74	31.38 ± 8.97	n.s.
Gender, Males, n (%)	107 (67.7 %)	61 (70.1 %)	46 (64.8 %)	n.s.
Deficit Syndrome, n (%)	41 (25.9)	29 (33.3)	12 (16.9)	χ^2 (1158) = 5.49, p = 0.019
Illness duration, years	6.49 ± 7.36	8.36 ± 8.10	4.21 ± 5.61	*t*(152.28) = 3.79, p < 0.001
Antipsychotic dose, CPZ eq mg/day	206.47 ± 185.26	227.41 ± 215.34	178.52 ± 134.32	n.s.
PANSS total score	40.4 ± 8.9	39.76 ± 8.86	41.18 ± 8.93	n.s.
PANSS positive subscale score	10.8 ± 3.9	10.43 ± 3.95	11.15 ± 3.91	n.s.
PANSS negative subscale score	9.1 ± 3.0	9.34 ± 3.38	8.76 ± 2.57	n.s.
PANSS GPS subscale score	20.6 ± 4.1	19.99 ± 3.74	21.27 ± 4.52	n.s.
GAF total score	50.9 ± 18.2	52.60 ± 17.59	48.84 ± 18.74	n.s.

Abbreviations: CPZ eq = Chlorpromazine equivalents; GAF = Global Assessment of Functioning; GPS = General Psychopathology; PANSS = Positive and Negative Syndrome Scale; SCZ = Schizophrenia; SG-1 = Schizophrenia subtype 1; SG-2 = Schizophrenia subtype 2.

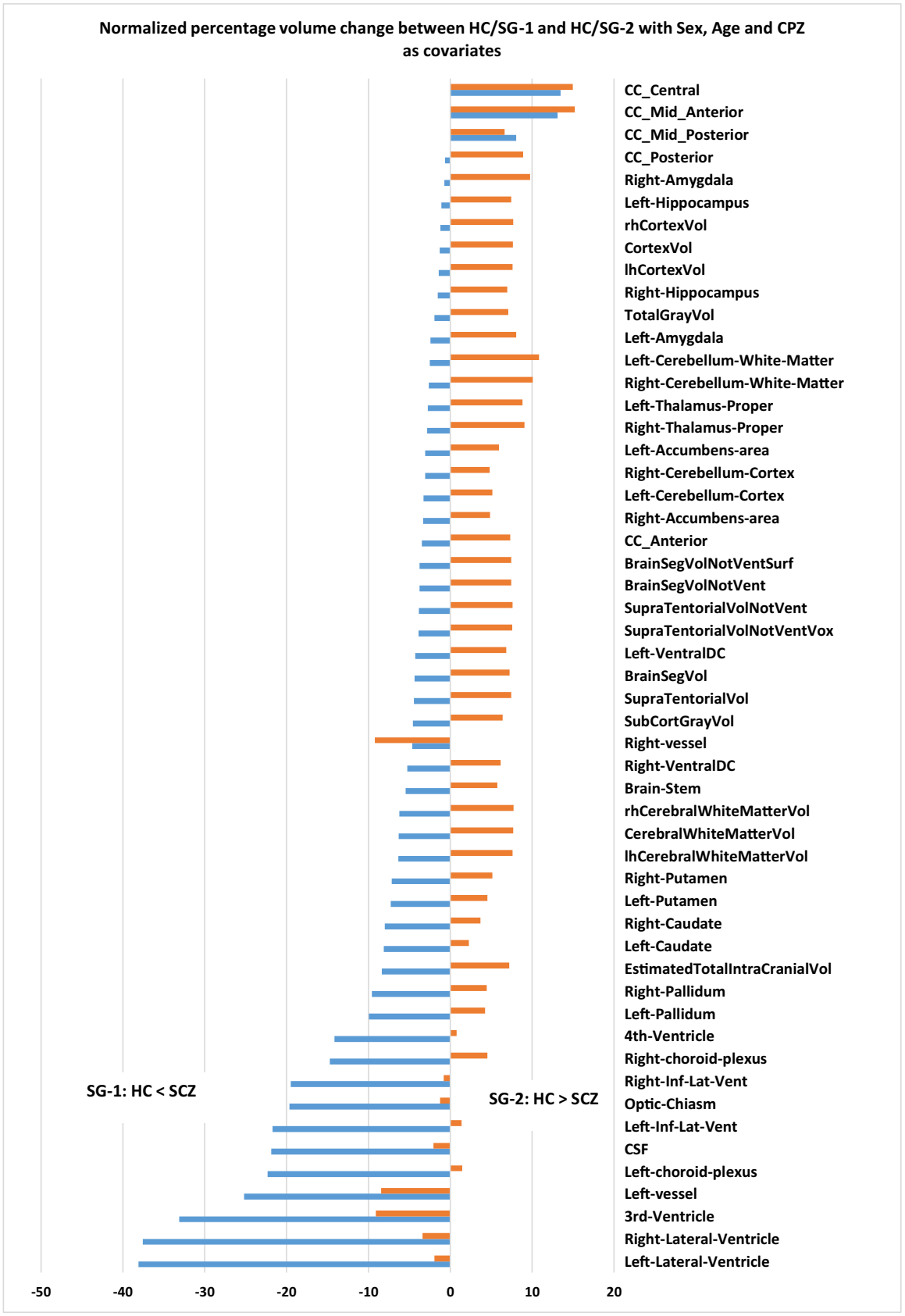

Fig. 1. Normalized percentage brain volume differences between Healthy Controls (HC) and neuroanatomical subtype SG-1, and HC and Subtype SG-2. Blue bars indicate subtype SG-1 structural volume changes whilst orange bars indicate SG-2 subtype volume changes. The negative x-axis represents volume increase (HC < SCZ) and positive x-axis indicate volume decrease (HC > SCZ). (For interpretation of the references to colour in this figure legend, the reader is referred to the web version of this article.)

observed reduced caudate volume in SCZ patients with deficit symptoms compared with HCs (Li et al., 2018). Smaller right putamen volume (Cascella et al., 2010) has been found in patients with deficit syndrome. However, earlier studies had also reported no significant changes of these structures (e.g Galderisi et al., 2008; Voineskos et al., 2013). Differences in medication status in initiation and use over time (Kirschner et al., 2021; van erp et al., 2016) could possibly serve to explain the contrasting findings involving the basal ganglia when compared to our study. Of note, medication-naïve SCZ patients have been found to have normal (Gur et al., 1998) or even decreased basal ganglia volumes (Keshavan et al., 1998; Corson et al., 1999). Regarding medications, typical antipsychotic drugs have been most often associated with volume increases compared with atypical antipsychotic drugs (Andersson et al., 2002; Lang et al., 2004).

The widespread reduction of cortical and subcortical brain volumes associated with SG-2 are consistent with earlier biological findings underlying SCZ. The nucleus accumbens (Fan et al., 2019; Mamah et al., 2007), amygdala, (Fan et al., 2019), thalamus (Yue et al., 2016), and hippocampal subfield volumes (Kühn et al., 2012) have been inversely associated with psychotic symptoms. In particular, specific hippocampal subfields are proposed to act as a binding module for cortical circuits containing weakly related sensory representations, such as the creation of representations of space and time which act as a basis of conscious awareness (Behrendt, 2010). Dysfunctions in these hippocampal subfields could result in abnormal integration of sensory representations which potentially manifests as psychotic symptoms (Tamminga et al., 2010). It has also been suggested that the disinhibition of subfields can cause hyperdopaminergic states which in turn produce psychosis (Lisman et al., 2008). Of note, volume reductions of corpus callosum were found in both neuroanatomical subtypes which are consistent with the findings of earlier reports (Collinson et al., 2014; Mitelman et al., 2009). Collinson et al. (2014) reported volume reductions of corpus callosum which were greatest in patients whose condition was chronic relative to patients with a first episode whilst Mitelman et al. (2009) reported similar reductions of absolute size of corpus callosum in SCZ compared with healthy controls over illness course longitudinally. In addition, deficit status in SCZ is linked with poor functional outcome (Galderisi et al., 2018), and poor outcome in SCZ has been associated with smaller callosal size compared with patients with better outcome (Mitelman et al., 2009).

In the present study, neural substrates have guided our classification of SCZ, offering clues to the neurobiology of the clinical features associated with SCZ such as illness duration, and deficit status. These findings have clinical implications in at least three main areas, namely early intervention, response monitoring, and prognosis. First, for earlier intervention, neurobiological features associated with SCZ can be used to assist in identification of subtypes of patients at variable duration of illness and clinical presentation even if history is unreliable or unavailable. For example, the presence of ventricular enlargement in a hitherto untreated patient may indicate long duration of illness including duration of untreated psychosis. Earlier treatment and improvement of illness psychopathology potentially can facilitate better illness remission (Correll et al., 2018), mitigate against longer term impact with illness chronicity especially if the condition is left untreated (Penttilä et al., 2014), improve functioning which can in turn reduce the burden of illness (Ruggeri et al., 2015). Second, for response monitoring, neurobiological features within subtypes can be monitored over time to evaluate the response of these structures to treatment. For example, within subtype SG-2, patients who are found with reductions of germane cortical (eg cortical white matter) or subcortical regions (eg hippocampus, thalamus), and absence of deficit status may indicate responsiveness to antipsychotic treatment which should be initiated appropriately. Third, for prognosis, observable neural markers or lack thereof can guide prognostication for our patients seen clinically (Dazzan, 2014; Keshavan et al., 2020; McGuire and Dazzan, 2017). For example, the absence of third and lateral ventricular enlargement in an older patient may portend a better prognosis compared with a younger patient with corresponding ventricular enlargement and who also has deficit presentation of avolition and social withdrawal.

There were several limitations to our study. First, our study had a modest sample size and it was cross-sectional in nature. Thus we were unable to report changes of neuroanatomical membership that may be observed over time in terms of subtypes. Second, subtyping was based on brain volume without the inclusion of other parameters such as cortical thickness, shape changes which could potentially have further enriched our understanding of the relationship between the neuroanatomical subtypes and clinical phenotypes. Third, we relied on a single imaging modality to identify neurobiological parameters for analysis. Future studies may look into the optimal number of subtypes in a larger cohort of SCZ and HC participants, examine the relationship of further subtypes with other clinical features such as cognition, functioning, as well as adopting a multi-modal neuroimaging approach to enhance insights into the neurobiological composition of the subtypes.

5. Conclusion

In summary, using a robust clustering classification framework, we replicated two neuroanatomical subtypes which were associated with specific clinical phenotypes. Further larger studies adopting a multimodality imaging approach may look into how different neural substrates are associated with other clinical features such as cognitive and psychosocial functioning, with potential implications for illness management and prognostication.

Declaration of competing interest

None.

Acknowledgements

This work was supported by National Healthcare Group (NHG), Singapore (SIG/05004) and Singapore Bioimaging Consortium (SBIC) (RP C-009/2006) research grants awarded to KS. The computational work for this article was partially performed on resources of the National Supercomputing Centre, Singapore (https://www.nscc.sg).

References

Alnæs, D., Kaufmann, T., van der Meer, D., Córdova-Palomera, A., Rokicki, J., Moberget, T., Karolinska Schizophrenia Project Consortium, 2019. Brain heterogeneity in schizophrenia and its association with polygenic risk. JAMA Psychiatry 76 (7), 739–748. https://doi.org/10.1001/jamapsychiatry.2019.0257.

Andersson, C., Hamer, R.M., Lawler, C.P., Mailman, R.B., Lieberman, J.A., 2002. Striatal volume changes in the rat following long-term administration of typical and atypical antipsychotic drugs. Neuropsychopharmacology 27 (2), 143–151. https://doi.org/10.1016/S0893-133X(02)00287-7.

Andreasen, N.C., Olsen, S.A., Dennert, J.W., Smith, M.R., 1982. Ventricular enlargement in schizophrenia: relationship to positive and negative symptoms. Am. J. Psychiatry 139 (3), 297–302.

Arnedo, J., Svrakic, D.M., Del Val, C., Romero-Zaliz, R., Hernández-Cuervo, H., , Molecular Genetics of Schizophrenia Consortium, Zwir, I., 2015. Uncovering the hidden risk architecture of the schizophrenias: confirmation in three independent genome-wide association studies. American Journal of Psychiatry 172 (2), 139–153. https://doi.org/10.1176/appi.ajp.2014.14040435.

Ballmaier, M., Schlagenhauf, F., Toga, A.W., et al., 2008. Regional patterns and clinical correlates of basal ganglia morphology in non-medicated schizophrenia. Schizophr. Res. 106 (2–3), 140–147. https://doi.org/10.1016/j.schres.2008.08.025.

Behrendt, R.P., 2010. Contribution of hippocampal region CA3 to consciousness and schizophrenic hallucinations. Neurosci. Biobehav. Rev. 34 (8), 1121–1136. https://doi.org/10.1016/j.neubiorev.2009.12.009.

Borgwardt, S.J., Smieskova, R., Fusar-Poli, P., Bendfeldt, K., Riecher-Rössler, A., 2009. The effects of antipsychotics on brain structure: what have we learnt from structural imaging of schizophrenia? Psychol. Med. 39 (11), 1781–1782. https://doi.org/10.1017/S0033291709006060.

Bragulat, V., Paillère-Martinot, M.L., Artiges, E., Frouin, V., Poline, J.B., Martinot, J.L., 2007. Dopaminergic function in depressed patients with affective flattening or with impulsivity: [18F]fluoro-L-dopa positron emission tomography study with voxel-based analysis. Psychiatry Res. 154 (2), 115–124. https://doi.org/10.1016/j.pscychresns.2006.07.002.

Brown, R., Colter, N., Corsellis, J.A., Crow, T.J., Frith, C.D., Jagoe, R., Marsh, L., 1986. Postmortem evidence of structural brain changes in schizophrenia. Differences in brain weight, temporal horn area, and parahippocampal gyrus compared with affective disorder. Arch. Gen. Psychiatry 43 (1), 36–42. https://doi.org/10.1001/archpsyc.1986.01800010038005.

Cascella, N.G., Fieldstone, S.C., Rao, V.A., Pearlson, G.D., Sawa, A., Schretlen, D.J., 2010. Gray-matter abnormalities in deficit schizophrenia. Schizophr. Res. 120 (1–3), 63–70. https://doi.org/10.1016/j.schres.2010.03.039.

Chand, G.B., Dwyer, D.B., Erus, G., Sotiras, A., Varol, E., Srinivasan, D., Davatzikos, C., 2020. Two distinct neuroanatomical subtypes of schizophrenia revealed using machine learning. Brain 143 (3), 1027–1038. https://doi.org/10.1093/brain/awaa025.

Chin, R., You, A.X., Meng, F., Zhou, J., Sim, K., 2018. Recognition of schizophrenia with regularized support vector machine and sequential region of interest selection using structural magnetic resonance imaging. Sci. Rep. 8 (1), 13858. https://doi.org/10.1038/s41598-018-32290-9.

Clementz, B.A., Sweeney, J.A., Hamm, J.P., Ivleva, E.I., Ethridge, L.E., Pearlson, G.D., Tamminga, C.A., 2016. Identification of distinct psychosis biotypes using brain-based biomarkers. Am. J. Psychiatry 173 (4), 373–384. https://doi.org/10.1176/appi.ajp.2015.14091200.

Collinson, S.L., Gan, S.C., Woon, P.S., Kuswanto, C., Sum, M.Y., Yang, G.L., Sim, K., 2014. Corpus callosum morphology in first-episode and chronic schizophrenia: combined magnetic resonance and diffusion tensor imaging study of chinese singaporean patients. Br. J. Psychiatry 204 (1), 55–60.

Correll, C.U., Galling, B., Pawar, A., Krivko, A., Bonetto, C., Ruggeri, M., Kane, J.M., 2018. Comparison of early intervention services vs treatment as usual for early-phase psychosis: a systematic review, meta-analysis, and meta-regression. JAMA Psychiatry 75 (6), 555–565. https://doi.org/10.1001/jamapsychiatry.2018.0623.

Corson, P.W., Nopoulos, P., Andreasen, N.C, Heckel, D., Arndt, S., 1999 Sep 1. Caudate size in first-episode neuroleptic-naive schizophrenic patients measured using an artificial neural network. Biol. Psychiatry 46 (5), 712–720.

Crow, T.J., 1985. The two-syndrome concept: origins and current status. Schizophr. Bull. 11 (3), 471–486. https://doi.org/10.1093/schbul/11.3.471.

Dazzan, P., 2014. Neuroimaging biomarkers to predict treatment response in schizophrenia: the end of 30 years of solitude? Dialogues Clin. Neurosci. 16 (4), 491–503. https://doi.org/10.31887/DCNS.2014.16.4/pdazzan.

Du, Y., Pearlson, G.D., Liu, J., Sui, J., Yu, Q., He, H., Calhoun, V.D., 2015. A group ICA based framework for evaluating resting fMRI markers when disease categories are unclear: application to schizophrenia, bipolar, and schizoaffective disorders. NeuroImage 122, 272–280. https://doi.org/10.1016/j.neuroimage.2015.07.054.

Dunn, R.T., Kimbrell, T.A., Ketter, T.A., Frye, M.A., Willis, M.W., Luckenbaugh, D.A., Post, R.M., 2002. Principal components of the Beck depression inventory and regional cerebral metabolism in unipolar and bipolar depression. Biol. Psychiatry 51 (5), 387–399. https://doi.org/10.1016/s0006-3223(01)01244-6.

Dwyer, D.B., Cabral, C., Kambeitz-Ilankovic, L., Sanfelici, R., Kambeitz, J., Calhoun, V., Koutsouleris, N., 2018. Brain subtyping enhances the neuroanatomical discrimination of schizophrenia. Schizophr. Bull. 44 (5), 1060–1069. https://doi.org/10.1093/schbul/sby008.

Fan, F., Xiang, H., Tan, S., Yang, F., Fan, H., Guo, H., Tan, Y., 2019. Subcortical structures and cognitive dysfunction in first episode schizophrenia. Psychiatry Res. Neuroimaging 286, 69–75. https://doi.org/10.1016/j.pscychresns.2019.01.003.

Fenton, W.S., McGlashan, T.H., 1994. Antecedents, symptom progression, and long-term outcome of the deficit syndrome in schizophrenia. Am. J. Psychiatry 151 (3), 351–356. https://doi.org/10.1176/ajp.151.3.351.

First, M.B., Spitzer, R.L., Gibbon, M., Williams, J.B.W., 1994a. Structured Clinical Interview for DSM-IV-TR Axis I Disorders, Research Version, Patient Edition (SCID-I/P). Biometrics Research, New York State Psychiatric Institute, New York, NY.

First, M.B., Spitzer, R.L., Gibbon, M., Williams, J.B.W., 1994b. Structured Clinical Interview for DSM-IV-TR Axis I Disorders, Research Version, Non-patient Edition (SCID-I/NP). Biometrics Research, New York State Psychiatric Institute, New York, NY.

Fischl, B., Sereno, M.I., Dale, A.M., 1999. Cortical surface-based analysis. II: inflation, flattening, and a surface-based coordinate system. NeuroImage 9 (2), 195–207. https://doi.org/10.1006/nimg.1998.0396.

Fischl, B., Salat, D.H., van der Kouwe, A.J., Makris, N., Ségonne, F., Quinn, B.T., Dale, A. M., 2004. Sequence-independent segmentation of magnetic resonance images. NeuroImage 23 (Suppl. 1), S69–S84. https://doi.org/10.1016/j.neuroimage.2004.07.016.

Galderisi, S., Quarantelli, M., Volpe, U., Mucci, A., Cassano, G.B., Invernizzi, G., Maj, M., 2008. Patterns of structural MRI abnormalities in deficit and nondeficit schizophrenia. Schizophr. Bull. 34 (2), 393–401. https://doi.org/10.1093/schbul/sbm097.

Galderisi, S., Mucci, A., Buchanan, R.W., Arango, C., 2018. Negative symptoms of schizophrenia: new developments and unanswered research questions. Lancet Psychiatry 5 (8), 664–677.

GBD 2017 Disease and Injury Incidence and Prevalence Collaborators, 2018. Global, regional, and national incidence, prevalence, and years lived with disability for 354 diseases and injuries for 195 countries and territories, 1990-2017: a systematic analysis for the Global Burden of Disease Study 2017. Lancet (London, England) 392 (10159), 1789–1858. https://doi.org/10.1016/S0140-6736(18)32279-7.

Goetz, R.R., Corcoran, C., Yale, S., et al., 2007. Validity of a 'proxy' for the deficit syndrome derived from the Positive And Negative Syndrome Scale (PANSS). Schizophr. Res. 93 (1–3), 169–177. https://doi.org/10.1016/j.schres.2007.02.018.

Goldsmith, D.R., Rapaport, M.H., 2020. Inflammation and negative symptoms of schizophrenia: implications for reward processing and motivational deficits. Front. Psychiatry 11, 46. https://doi.org/10.3389/fpsyt.2020.00046.

Gur, R.E., Maany, V., Mozley, P.D., Swanson, C., Bilker, W., Gur, R.C., 1998 Dec. Subcortical MRI volumes in neuroleptic-naive and treated patients with schizophrenia. Am. J. Psychiatry 155 (12), 1711-7.

Ho, N.F., Lee, B., Tng, J., Lam, M., Chen, G., Wang, M., Sim, K., 2020. Corticolimbic brain anomalies are associated with cognitive subtypes in psychosis: a longitudinal study. Eur. Psychiatry 63 (1), e40. https://doi.org/10.1192/j.eurpsy.2020.36.

Hu, M., Qian, X., Liu, S., Koh, A.J., Sim, K., Jiang, X., Zhou, J.H., 2021. Structural and diffusion MRI based schizophrenia classification using 2D pretrained and 3D naive Convolutional Neural Networks, 0920-9964(21)00223-1 Schizophr. Research. https://doi.org/10.1016/j.schres.2021.06.011. Advance online publication.

Huber, G., 1997. The heterogeneous course of schizophrenia. Schizophr. Res. 28 (2–3), 177–185. https://doi.org/10.1016/s0920-9964(97)00113-8.

Ivleva, E.I., Bidesi, A.S., Thomas, B.P., Meda, S.A., Francis, A., Moates, A.F., Tamminga, C.A., 2012. Brain gray matter phenotypes across the psychosis dimension. Psychiatry Res. 204 (1), 13–24. https://doi.org/10.1016/j.pscychresns.2012.05.001.

JMP®, 1989–2021. Version 12. SAS Institute Inc., Cary, NC.

Kay, S.R., Fiszbein, A., Opler, L.A., 1987. The positive and negative syndrome scale (PANSS) for schizophrenia. Schizophr. Bull 13 (2), 261–276. https://doi.org/10.1093/schbul/13.2.261.

Keshavan, M.S., Collin, G., Guimond, S., Kelly, S., Prasad, K.M., Lizano, P., 2020. Neuroimaging in schizophrenia. Neuroimaging Clin. N. Am. 30 (1), 73–83. https://doi.org/10.1016/j.nic.2019.09.007.

Keshavan, M.S., Rosenberg, D., Sweeney, J.A., Pettegrew, J.W., 1998 Jun. Decreased caudate volume in neuroleptic-naive psychotic patients. Am. J. Psychiatry 155 (6), 774-8.

Killgore, W.D., Rosso, I.M., Gruber, S.A., Yurgelun-Todd, D.A., 2009. Amygdala volume and verbal memory performance in schizophrenia and bipolar disorder. Cogn. Behav. Neurol. 22 (1), 28–37. https://doi.org/10.1097/WNN.0b013e318192cc67.

Kirkpatrick, B., Buchanan, R.W., Breier, A., Carpenter Jr., W.T., 1993. Case identification and stability of the deficit syndrome of schizophrenia. Psychiatry Res. 47 (1), 47–56. https://doi.org/10.1016/0165-1781(93)90054-k.

Kirschner, M., Schmidt, A., Hodzic-Santor, B., Burrer, A., Manoliu, A., Zeighami, Y., Kaiser, S., 2021. Orbitofrontal-striatal structural alterations linked to negative symptoms at different stages of the schizophrenia spectrum. Schizophr. Bull. 47 (3), 849–863. https://doi.org/10.1093/schbul/sbaa169.

Kühn, S., Musso, F., Mobascher, A., Warbrick, T., Winterer, G., Gallinat, J., 2012. Hippocampal subfields predict positive symptoms in schizophrenia: first evidence from brain morphometry. Transl. Psychiatry 2 (6), e127. https://doi.org/10.1038/tp.2012.51.

Lakhan, S.E., Vieira, K.F., 2009. Schizophrenia pathophysiology: are we any closer to a complete model? Ann. General Psychiatry 8, 12. https://doi.org/10.1186/1744-859X-8-12.

Lang, D.J., Kopala, L.C., Vandorpe, R.A., Rui, Q., Smith, G.N., Goghari, V.M., Honer, W. G., 2004. Reduced basal ganglia volumes after switching to olanzapine in chronically treated patients with schizophrenia. Am. J. Psychiatry 161 (10), 1829–1836. https://doi.org/10.1176/ajp.161.10.1829.

Li, Y., Li, W.X., Xie, D.J., Wang, Y., Cheung, E., Chan, R., 2018. Grey matter reduction in the caudate nucleus in patients with persistent negative symptoms: an ALE meta-analysis. Schizophr. Res. 192, 9–15. https://doi.org/10.1016/j.schres.2017.04.005.

Lisman, J.E., Coyle, J.T., Green, R.W., Javitt, D.C., Benes, F.M., Heckers, S., Grace, A.A., 2008. Circuit-based framework for understanding neurotransmitter and risk gene interactions in schizophrenia. Trends Neurosci. 31 (5), 234–242. https://doi.org/10.1016/j.tins.2008.02.005.

Malhotra, A.K., 2015. Dissecting the heterogeneity of treatment response in first-episode schizophrenia. Schizophr. Bull. 41 (6), 1224–1226. https://doi.org/10.1093/schbul/sbv117.

Mamah, D., Wang, L., Barch, D., de Erausquin, G.A., Gado, M., Csernansky, J.G., 2007. Structural analysis of the basal ganglia in schizophrenia. Schizophr. Res. 89 (1–3), 59–71. https://doi.org/10.1016/j.schres.2006.08.031.

McGuire, P., Dazzan, P., 2017. Does neuroimaging have a role in predicting outcomes in psychosis? World Psychiatry 16 (2), 209–210. https://doi.org/10.1002/wps.20426.

Mitelman, S.A., Nikiforova, Y.K., Canfield, E.L., Hazlett, E.A., Brickman, A.M., Shihabuddin, L., Buchsbaum, M.S., 2009. A longitudinal study of the corpus callosum in chronic schizophrenia. Schizophr. Res. 114 (1–3), 144–153.

Oh, K., Kim, W., Shen, G., Piao, Y., Kang, N.I., Oh, I.S., Chung, Y.C., 2019. Classification of schizophrenia and normal controls using 3D convolutional neural network and outcome visualization. Schizophr. Res. 212, 186–195. https://doi.org/10.1016/j.schres.2019.07.034.

Okada, N., Fukunaga, M., Yamashita, F., Koshiyama, D., Yamamori, H., Ohi, K., Hashimoto, R., 2016. Abnormal asymmetries in subcortical brain volume in schizophrenia. Mol. Psychiatry 21 (10), 1460–1466. https://doi.org/10.1038/mp.2015.209.

Penttilä, M., Jääskeläinen, E., Hirvonen, N., Isohanni, M., Miettunen, J., 2014. Duration of untreated psychosis as predictor of long-term outcome in schizophrenia: systematic review and meta-analysis. Br. J. Psychiatry 205 (2), 88–94. https://doi.org/10.1192/bjp.bp.113.127753.

Pina-Camacho, L., Del Rey-Mejías, Á., Janssen, J., Bioque, M., González-Pinto, A., Arango, C., PEPs Group, 2016. Age at first episode modulates diagnosis-related structural brain abnormalities in psychosis. Schizophrenia Bulletin 42 (2), 344–357. https://doi.org/10.1093/schbul/sbv128.

Plailly, J., d'Amato, T., Saoud, M., Royet, J.P., 2006. Left temporo-limbic and orbital dysfunction in schizophrenia during odor familiarity and hedonicity judgments. NeuroImage 29 (1), 302–313. https://doi.org/10.1016/j.neuroimage.2005.06.056.

R Core Team, 2020. R: A Language and Environment for Statistical Computing. R Foundation for Statistical Computing, Vienna, Austria. https://www.R-project.org/.

RStudio Team (2020). RStudio: Integrated Development for R. RStudio, PBC, Boston, MA URL http://www.rstudio.com/.
Ruggeri, M., Bonetto, C., Lasalvia, A., Fioritti, A., de Girolamo, G., Santonastaso, P., GET UP Group, 2015. Feasibility and effectiveness of a multi-element psychosocial intervention for first-episode psychosis: results from the cluster-randomized controlled GET UP PIANO trial in a catchment area of 10 million inhabitants. Schizophrenia Bulletin 41 (5), 1192–1203. https://doi.org/10.1093/schbul/sbv058.
Sandyk, R., 1993. Third ventricular width and its relationship to mode of onset of schizophrenia. Int. J. Neurosci. 69 (1–4), 119–124. https://doi.org/10.3109/00207459309003321.
Seaton, B.E., Goldstein, G., Allen, D.N., 2001. Sources of heterogeneity in schizophrenia: the role of neuropsychological functioning. Neuropsychol. Rev. 11 (1), 45–67. https://doi.org/10.1023/a:1009013718684.
Sum, M.Y., Tay, K.H., Sengupta, S., Sim, K., 2018. Neurocognitive functioning and quality of life in patients with and without deficit syndrome of schizophrenia. Psychiatry Res. 263, 54–60. https://doi.org/10.1016/j.psychres.2018.02.025.
Tamminga, C.A., Stan, A.D., Wagner, A.D., 2010. The hippocampal formation in schizophrenia. Am. J. Psychiatry 167 (10), 1178–1193. https://doi.org/10.1176/appi.ajp.2010.09081187.
Tan, A.S., Chew, Q.H., Sim, K., 2020. Cerebral white matter changes in deficit and non-deficit subtypes of schizophrenia. Journal of Neural Transmission (Vienna, Austria : 1996) 127 (7), 1073–1079. https://doi.org/10.1007/s00702-020-02207-w.
van Erp, T.G., Hibar, D.P., Rasmussen, J.M., Glahn, D.C., Pearlson, G.D., Andreassen, O. A., Turner, J.A., 2016. Subcortical brain volume abnormalities in 2028 individuals with schizophrenia and 2540 healthy controls via the ENIGMA consortium. Mol. Psychiatry 21 (4), 585. https://doi.org/10.1038/mp.2015.118.
Van Rheenen, T.E., Lewandowski, K.E., Tan, E.J., Ospina, L.H., Ongur, D., Neill, E., Burdick, K.E., 2017. Characterizing cognitive heterogeneity on the schizophrenia-bipolar disorder spectrum. Psychol. Med. 47 (10), 1848–1864. https://doi.org/10.1017/S0033291717000307.
Varol, E., Sotiras, A., Davatzikos, C., Alzheimer's Disease Neuroimaging Initiative, 2017. HYDRA: Revealing heterogeneity of imaging and genetic patterns through a multiple max-margin discriminative analysis framework. NeuroImage 145 (Pt B), 346–364. https://doi.org/10.1016/j.neuroimage.2016.02.041.
Voineskos, A.N., Foussias, G., Lerch, J., Felsky, D., Remington, G., Rajji, T.K., Mulsant, B. H., 2013. Neuroimaging evidence for the deficit subtype of schizophrenia. JAMA Psychiatry 70 (5), 472–480. https://doi.org/10.1001/jamapsychiatry.2013.786.
Voineskos, A.N., Jacobs, G.R., Ameis, S.H., 2020. Neuroimaging heterogeneity in psychosis: neurobiological underpinnings and opportunities for prognostic and therapeutic innovation. Biol. Psychiatry 88 (1), 95–102. https://doi.org/10.1016/j.biopsych.2019.09.004.
Weinberg, D., Lenroot, R., Jacomb, I., Allen, K., Bruggemann, J., Wells, R., Weickert, T. W., 2016. Cognitive subtypes of schizophrenia characterized by differential brain volumetric reductions and cognitive decline. JAMA Psychiatry 73 (12), 1251–1259. https://doi.org/10.1001/jamapsychiatry.2016.2925.
Weinberger, D.R., Torrey, E.F., Neophytides, A.N., Wyatt, R.J., 1979. Lateral cerebral ventricular enlargement in chronic schizophrenia. Arch. Gen. Psychiatry 36 (7), 735–739. https://doi.org/10.1001/archpsyc.1979.01780070013001.
Womer, F.Y., Wang, L., Alpert, K.I., Smith, M.J., Csernansky, J.G., Barch, D.M., Mamah, D., 2014. Basal ganglia and thalamic morphology in schizophrenia and bipolar disorder. Psychiatry Res. 223 (2), 75–83. https://doi.org/10.1016/j.pscychresns.2014.05.017.
Wong, H.J., Chew, Q.H., Lee, R.D., Sim, K., 2020. Illness remission status and commissural and associative brain white matter fiber changes in schizophrenia. PsyCh J. 9 (6), 894–902. https://doi.org/10.1002/pchj.399.
Yue, Y., Kong, L., Wang, J., Li, C., Tan, L., Su, H., Xu, Y., 2016. Regional abnormality of grey matter in schizophrenia: effect from the illness or treatment? PLoS One 11 (1), e0147204. https://doi.org/10.1371/journal.pone.0147204.